Single-cell photoacoustic thermometry

Liang Gao, Lidai Wang, Chiye Li, Yan Liu, Haixin Ke, et al.

Liang Gao, Lidai Wang, Chiye Li, Yan Liu, Haixin Ke, Chi Zhang, Lihong V. Wang , "Single-cell photoacoustic thermometry," Proc. SPIE 8581, Photons Plus Ultrasound: Imaging and Sensing 2013, 858118 (4 March 2013); doi: 10.1117/12.2004063

SPIE.

Event: SPIE BiOS, 2013, San Francisco, California, United States

Single-cell photoacoustic thermometry

Liang Gao, Lidai Wang, Chiye Li, Yan Liu, Haixin Ke, Chi Zhang, and Lihong V. Wang

Department of Biomedical Engineering, Washington University in St. Louis
One Brookings Dr., St. Louis, MO, 63130

ABSTRACT

A novel photoacoustic thermometric method is presented for simultaneously imaging cells and sensing their temperature. With 3 seconds per frame imaging speed, a temperature resolution of 0.2 ^{o}C was achieved in a photo-thermal cell heating experiment. Compared to other approaches, the photoacoustic thermometric method has the advantage of not requiring custom-developed temperature-sensitive biosensors. This feature should facilitate the conversion of single-cell thermometry into a routine lab tool and make it accessible to a much broader biological research community.

Keywords: Single-cell thermometry, temperature sensing, photoacoustic microscopy

1. INTRODUCTION

Cellular events – such as division, gene expression and enzyme reaction – are often accompanied by intracellular temperature changes[1]. Accurately measuring intracellular temperature may provide new insights into cellular signaling and metabolism. However, sensing intracellular temperature is not a trivial task, especially at the single cell level.

Currently, there are two major approaches to intracellular temperature sensing: one uses micro- or nano-scale thermocouples [2, 3]; the other employs temperature-sensitive fluorescent dyes [4], proteins [5], or nanoparticles [6]. Although the thermocouple-based approach features high temperature resolution (~0.1 ^{o}C [3]), to detect intracellular temperature changes, the tip of the thermocouple has to be inserted into cells via a micromanipulation system. This invasive operation may interrupt normal cell metabolic cycles and cause cell damage. In addition, only one cell can be measured at a time. On the other hand, the fluorescence-based approach realizes simultaneous imaging and temperature sensing with ~0.5 ^{o}C resolution [7]. However, most temperature-sensitive fluorescent biosensors present problems, such as sensitivity to solution pH values and potential toxicity to cells [8].

To overcome these limitations, we present a novel single-cell photoacoustic thermometric method for intracellular temperature sensing. The system is based on high-resolution photoacoustic microscopy (PAM), which measures ultrasound signals induced by light absorption. PAM has achieved diffraction-limited optical resolution, and been successfully applied in cellular imaging applications, e.g., detecting nanoparticle-targeted cancer cells [9] and label-free imaging of cell nuclei [10]. In PAM, the acquired photoacoustic (PA) image amplitude is proportional to the initial pressure rise p_0 at the absorber, induced by short-pulse laser excitation. The initial pressure rise is given by [11]

$$p_0 = (\frac{\beta v_s^2}{C_p})\mu_a F = \Gamma \mu_a F \,. \tag{1}$$

Here, β is the thermal expansion coefficient, v_s is the speed of sound in the medium, C_p is the specific heat capacity at constant pressure, μ_a is the optical absorption coefficient, and F is the optical fluence. The Gruneisen parameter Γ is temperature dependent in water, as given by the empirical relation

$$\Gamma = A + BT \,, \tag{2}$$

where A and B are constants, and T is the local temperature surrounding the absorber in degrees Celsius. Substituting Γ from Eq. 2 into Eq. 1 gives

$$p_0 = (A + BT)\mu_a F \,. \tag{3}$$

Consequently, by measuring the photoacoustic signal generated by the absorber, the local temperature can be detected. Although photoacoustic thermometry has been employed in evaluating biological tissue temperatures [12], to our knowledge, this is the first time it has been used for single cell temperature imaging.

Photons Plus Ultrasound: Imaging and Sensing 2013, edited by Alexander A. Oraevsky, Lihong V. Wang,
Proc. of SPIE Vol. 8581, 858118 · © 2013 SPIE · CCC code: 1605-7422/13/$18 · doi: 10.1117/12.2004063

2. SYSTEM DESCRIPTION

A recently developed voice-coil PAM system [13] (Fig. 1) was employed to acquire temperature-dependent cellular images. The voice-coil PAM system consisted of a PA probe and a raster scanner. In the PA probe, short laser pulses at 532 nm (10-200-532, Elforlight Ltd.) were focused onto the sample surface through a set of optics. The generated photoacoustic signals were collected by an ultrasound lens (6 mm aperture, 0.5 NA in water) and received by a high-frequency ultrasound transducer (V2022 BC, Olympus NDT). To achieve high sensitivity, the optical and acoustic foci were confocally and coaxially aligned. The photoacoustic probe was mounted onto a voice-coil-based scanner (VCS-1010, Equipment Solutions) to implement fast imaging.

In experiments, the sample was scanned at a 10 Hz cross sectional imaging speed and a 1/3 Hz volumetric imaging speed. The lateral resolution was measured as 3.4 μm. A higher spatial resolution is possible by increasing the optical numerical aperture.

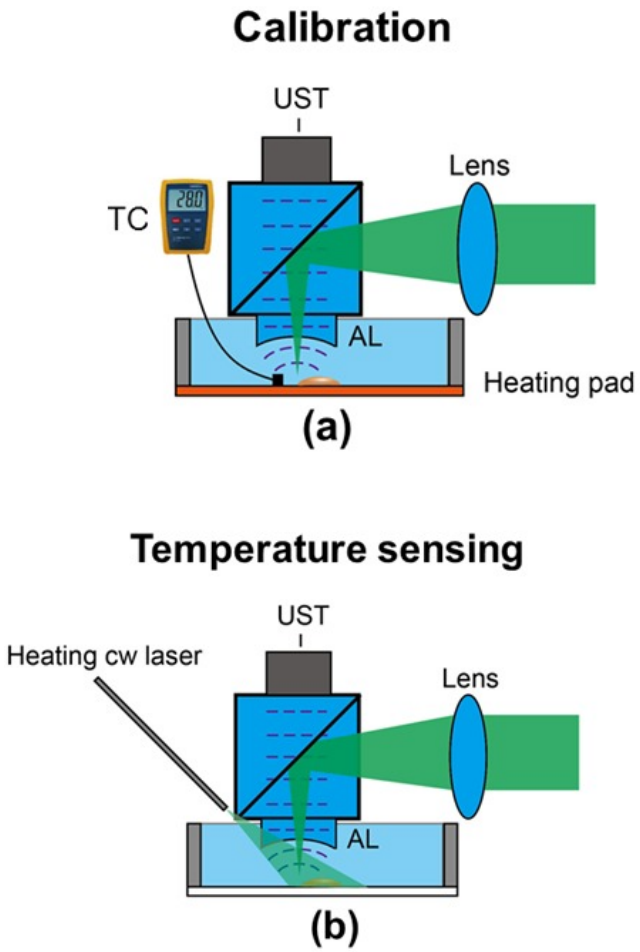

Fig. 1. System layout of PA-based cellular temperature sensing during (a) calibration and (b) photo-thermal heating. In (b), the cell was heated by a 100-mW CW laser via a multimode fiber. The intracellular temperature was monitored by a voice-coil PAM system in real time. AL, acoustic lens; UST, ultrasound transducer; TC, thermocouple.

2. RESULTS

To demonstrate single-cell photoacoustic thermometry, an intracellular temperature sensing experiment was carried out on HeLa cancer cells during photo-thermal heating. The HeLa cells were loaded with iron oxide micro-particles (mean diameter, 2.5 microns, PI21353, Fisher Scientific) as both a photoacoustic imaging contrast agent and a photo-thermal

heating source. The cells were immersed in PBS and imaged by the PAM. Laser pulse energy was recorded by a photodiode, and variations in the output were corrected pulse-by-pulse.

2.1 Sample preparison

The HeLa cells were maintained in Dulbecco's Modified Eagle Medium with 10% fetal bovine serum, 2 mM glutamine, and 1% penicillin/streptomycin supplement. The cells were incubated at 37 ^{o}C in 5% CO_2, and were divided every 72 hours. After being dispersed in 0.25% EDTA-trypsin, they were seeded at 2-4×104 cells/cm^2. As a PA imaging contrast agent, iron oxide micro-particles (PI21353, Fisher Scientific; 1 μm size) were added to the cell medium in a concentration of 0.5 pM and incubated for 24 hours. Coverslips with adherent cells were washed with PBS before imaging.

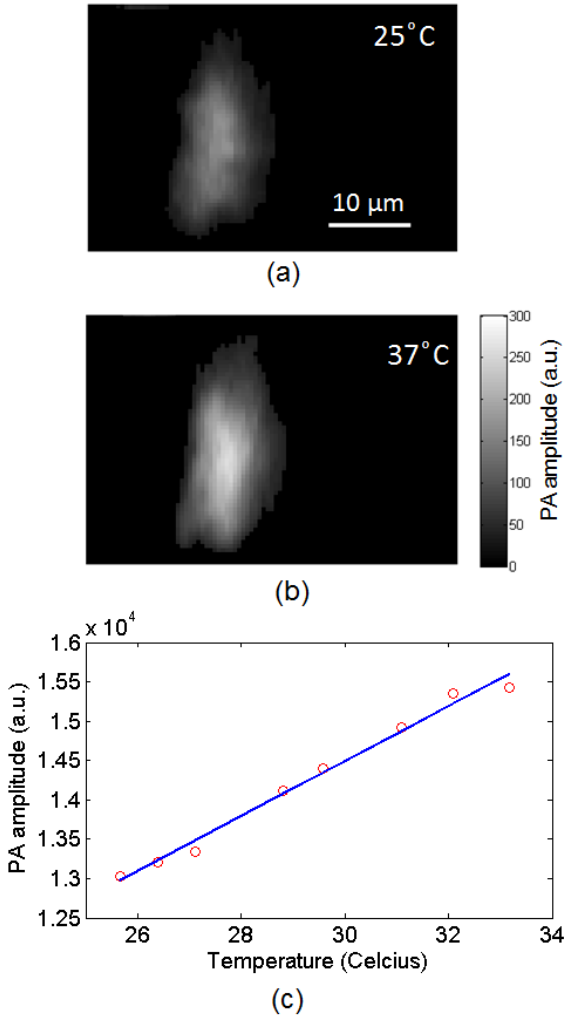

Fig. 2. PA-based single-cell thermometric calibration. (a) Cell image at 23 ^{o}C. (b) Cell image at 37 ^{o}C. (c) PA amplitude vs. temperature for the cell in (a). The coefficient of determination, R^2, was 0.994.

2.2 Calibration

To study the relationship between intracellular temperature and PA image amplitude, a coverslip with adherent HeLa cells was uniformly heated by a custom-made heating pad, as shown in Fig. 1(a). The heating pad was made by connecting a thin metallic platform to a resistive heater (HT10K, Thorlabs). A thermocouple was placed in contact with

the coverslip and close to (~ 1mm) the cells. The environment temperature was gradually raised by increasing the voltage applied to the heating pad. At each temperature, after enough time had elapsed to ensure that thermal equilibrium had been reached among the cells, the thermocouple, and the environment, a PA image was acquired and the temperature was measured by the thermocouple. Since the thermal and stress relaxation times for a 2.5 micron particle are 270 ns and 1.7 ns, respectively, which are longer than the laser pulse duration (~1 ns), both thermal and stress confinement conditions were satisfied. After fluence correction, the acquired PA image amplitude (peak-to-peak value of each A-line signal) was given by

$$S = k\frac{p_0}{F} = k\mu_a BT + k\mu_a A\,, \tag{4}$$

where k is the system's pressure sensitivity.

The measured PA signal vs. temperature for a single cell is shown in Fig. 2. The PA signal of the cell was calculated by averaging all pixels within the cellular boundary. The result indicates that the cellular temperature rise was accompanied by a linear increase in its PA signal. The slope $k\mu_a B$ and intercept $k\mu_a A$ thus could be solved by linear regression. Since the cellular temperature has a one-to-one correspondence to its PA signal, the PA-recovered cellular temperature was calculated as

$$T = \frac{I - k\mu_a A}{k\mu_a B}. \tag{5}$$

2.3 Single-cell temperature sensing during photo-thermal heating

Localized photo-thermal heating is widely used in cancer therapy. Measurement of cellular temperature during photo-thermal heating is important to understanding the thermodynamics of cancer cells. To simulate the heating process, the output from a 100-mW CW laser (MLL-III-532, General Optoelectronic) was guided to the sample by a multimode fiber (BFL37-600, Thorlabs) to heat the HeLa cancer cells (see Fig. 1(b)).

The experiment was divided into two steps. First, a control experiment without photo-thermal heating was performed to provide a baseline. The cellular temperature was monitored by the PAM at constant room temperature (Fig. 3). The image acquisition speed was 3 seconds per frame. With this imaging speed, the temperature resolution – defined as the standard deviation of the measured control temperature – was 0.2 ^{o}C. Note that by using a slower imaging speed or a finer imaging step size, the temperature resolution can be further improved. In the second step, the heating CW laser was turned on and the cellular temperature was continuously measured by the PAM at the same acquisition speed. As seen in Fig. 3, the PA-recovered cellular temperature rose from 23 ^{o}C to 26 ^{o}C during the 300 second heating period. After the heating laser was turned off, the cellular temperature gradually decreased to the room temperature.

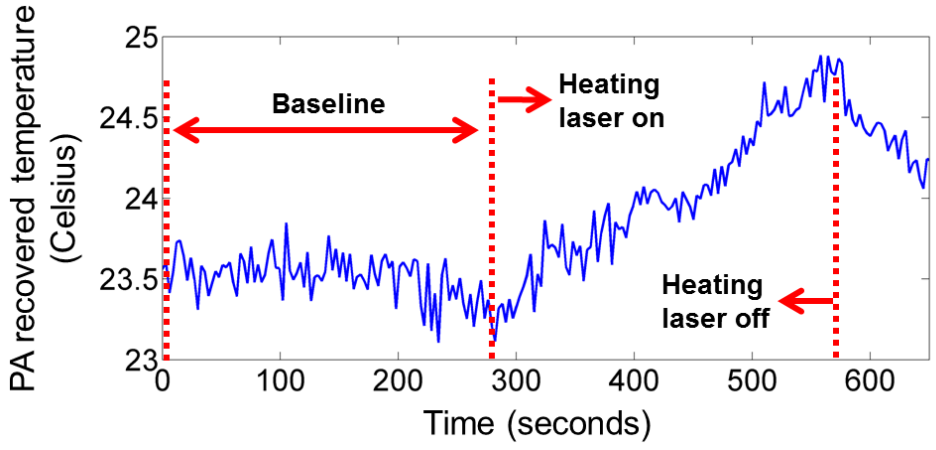

Fig. 3 Single cell temperature sensing during control and photo-thermal heating stages.

To test cells' viability after these procedures, the cells were stained with green-fluorescent calcein-AM (L-3224, Life Technologies, Inc.) to indicate intracellular esterase activity and red-fluorescent ethidium homodimer-1 to indicate loss

of plasma membrane integrity. The cells were re-imaged on a fluorescence microscope (Fig. 4), and the results show that > 80 % of cells were still viable after photoacoustic imaging.

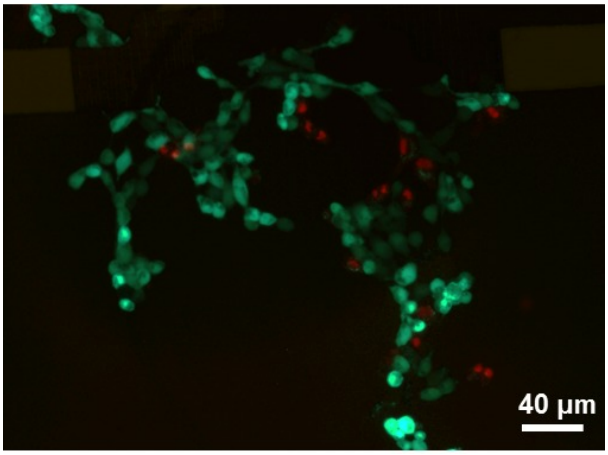

Fig. 4. Cellular viability test after photoacoustic imaging. Cells emitting green fluorescence are alive, while those emitting red fluorescence are dead.

3. DISCUSSION

During raster scanning, repetitive probe laser pulses may cause a local temperature rise. Here, this effect was estimated by using the laser specific parameters and a typical value of thermal diffusivity in water (1.4×10-7 m^2·s-1 at 25 ^oC). The calculation indicated that two adjacent laser pulses can raise the local temperature by as much as 0.1 ^oC. Summing ~1000 laser pulses scanning across a cell, the estimated total temperature rise was ~0.25 ^oC, which is much less than the cell temperature. If a smaller temperature rise is desired, lower laser pulse energy and a slower pulse repetition rate may be used.

We also evaluated the dependence of the system's pressure sensitivity on the coupling water's temperature. First, since the ultrasound transducer was in air and the room temperature was thermostatically controlled during the experiments, the transducer's pressure sensitivity could be considered constant. Next, because the coupling water's temperature change might alter the speed of sound, acoustic focal distance, and focal spot size, the system's pressure sensitivity could be affected. Here we estimated the acoustic focal distance and spot size at 25 ^oC and 33 ^oC, with an assumption of uniform temperature distribution in the coupling water. The focal distance was calculated from

$$l = \frac{v_q}{v_q - v_w} R \,, \tag{8}$$

where l is the focal distance, v_q is the sound speed in acoustic lens (quarts), v_w is the sound speed in water, and R is the radius of the acoustic lens. The focal diameter d is computed from

$$d = 0.71 \frac{v_w 2l}{fD} \,, \tag{9}$$

where f is the acoustic frequency, and D is the outer diameter of the acoustic lens. When temperature increased from 25 ^oC to 33 ^oC, the focal distance and the focal diameter decreased by 0.5% and 1.7%, respectively. By linear approximation, the total temperature's effect on the system sensitivity was estimated as $(1\text{-}0.005)\times(1+0.017)^2\text{-}1=2.9\%$. At the same time, the measured PA amplitude increased by 41%, which was 13 times higher than the system's pressure sensitivity change. Therefore the effect of the coupling water's temperature change on the system's pressure sensitivity was negligible.

The single-cell photoacoustic thermometry requires that the cell stays in the same solution and cellular environment during calibration and temperature measurement experiments. For *in-vivo* studies, since the tissue surrounding the cell may also contribute to the PA signal [14], the correspondence between PA amplitude and cellular temperature acquired by *in-vitro* calibration experiments may not be applicable. To reduce the effect of surrounding tissue on the *in-vivo*

cellular temperature measurement, one can minimize the ratio of the tissue's absorption to the sensing particle's absorption by choosing a specimen-specific wavelength.

4. CONCLUSION

In summary, a novel PAM-based method is presented for single-cell temperature sensing. With 3 seconds/frame imaging speed, the PAM-based method has achieved a temperature resolution of 0.2 ^{o}C in a photo-thermal heating experiment. To the best of our knowledge, this is the first time that photoacoustic temperature sensing has been realized at the single-cell level.

Compared to other cellular temperature sensing methods, the PAM-based approach has the advantage of not requiring custom-developed temperature-sensitive biosensors. One can choose commercially available absorptive dyes or particles as the temperature sensitive agent in cellular imaging applications. Although not demonstrated in this paper, by tuning the imaging laser wavelength, endogenous cellular absorption contrasts, such as hemoglobin, melanin, lipid, DNA/RNA, and protein, can also be employed for intracellular temperature sensing without cellular staining. The presented photoacoustic thermometry should make single-cell temperature sensing accessible to a much broader biological research community.

ACKNOWLEDGMENTS

This work was sponsored by the National Institutes of Health (NIH) under grants R01 EB000712, R01 EB008085, R01 CA134539, U54 CA136398, R01 CA157277, R01 CA159959 and DP1 EB016986. L. V. Wang has a financial interest in Microphotoacoustics, Inc. and Endra, Inc.; however, neither provided support for this work.

REFERENCES

1. B. B. Lowell and B. M. Spiegelman, "Towards a molecular understanding of adaptive thermogenesis," *Nature* 404(6778), 652-660 (2000)
2. M. Suzuki, V. Tseeb, K. Oyama and S. Ishiwata, "Microscopic detection of thermogenesis in a single HeLa cell," *Biophys J* 92(6), L46-L48 (2007)
3. C. L. Wang, R. Z. Xu, W. J. Tian, X. L. Jiang, Z. Y. Cui, M. Wang, H. M. Sun, K. Fang and N. Gu, "Determining intracellular temperature at single-cell level by a novel thermocouple method," *Cell Res* 21(10), 1517-1519 (2011)
4. C. F. Chapman, Y. Liu, G. J. Sonek and B. J. Tromberg, "The Use of Exogenous Fluorescent-Probes for Temperature-Measurements in Single Living Cells," *Photochem Photobiol* 62(3), 416-425 (1995)
5. J. S. Donner, S. A. Thompson, M. P. Kreuzer, G. Baffou and R. Quidant, "Mapping Intracellular Temperature Using Green Fluorescent Protein," *Nano Lett* 12(4), 2107-2111 (2012)
6. F. Vetrone, R. Naccache, A. Zamarron, A. J. de la Fuente, F. Sanz-Rodriguez, L. M. Maestro, E. M. Rodriguez, D. Jaque, J. G. Sole and J. A. Capobianco, "Temperature Sensing Using Fluorescent Nanothermometers," *Acs Nano* 4(6), 3254-3258 (2010)
7. C. Gota, K. Okabe, T. Funatsu, Y. Harada and S. Uchiyama, "Hydrophilic Fluorescent Nanogel Thermometer for Intracellular Thermometry," *J Am Chem Soc* 131(8), 2766-2767 (2009)
8. O. Zohar, M. Ikeda, H. Shinagawa, H. Inoue, H. Nakamura, D. Elbaum, D. L. Alkon and T. Yoshioka, "Thermal imaging of receptor-activated heat production in single cells," *Biophys J* 74(1), 82-89 (1998)
9. S. Mallidi, T. Larson, J. Tam, P. P. Joshi, A. Karpiouk, K. Sokolov and S. Emelianov, "Multiwavelength Photoacoustic Imaging and Plasmon Resonance Coupling of Gold Nanoparticles for Selective Detection of Cancer," *Nano Lett* 9(8), 2825-2831 (2009)
10. D. K. Yao, K. Maslov, K. K. Shung, Q. F. Zhou and L. V. Wang, "In vivo label-free photoacoustic microscopy of cell nuclei by excitation of DNA and RNA," *Optics Letters* 35(24), 4139-4141 (2010)
11. L. V. Wang and H.-i. Wu, *Biomedical optics : principles and imaging*, Wiley-Interscience, Hoboken, N.J. (2007).
12. I. V. Larina, K. V. Larin and R. O. Esenaliev, "Real-time optoacoustic monitoring of temperature in tissues," *J Phys D Appl Phys* 38(15), 2633-2639 (2005)
13. L. D. Wang, K. Maslov, J. J. Yao, B. Rao and L. H. V. Wang, "Fast voice-coil scanning optical-resolution photoacoustic microscopy," *Optics Letters* 36(2), 139-141 (2011)
14. V. N. Inkov, A. A. Karabutov and I. M. Pelivanov, "A theoretical model of the linear thermo-optical response of an absorbing particle immersed in a liquid," *Laser Phys* 11(12), 1283-1291 (2001)